Orthogonal Rotation Invariant Moments and Transforms for Pattern Recognition and Computer Vision Applications

Rahul Upneja[1], Ali Mohammed Sahan[2]

Assistant Professor, Sri Guru Granth Sahib World University, Fatehgarh Sahib[1]

Department of Information Technology, Meddle Technical University, Baghdad, Iraq[2]

Abstract— **Various radial moments and polar harmonic transforms such as polar complex exponential transforms, polar cosine transforms and polar sine transforms satisfy orthogonal principle. By virtue of which these moments and transforms possess minimum information redundancy and thereby exhibit a good characteristic of image representation. In this paper, a complete comparative analysis is performed by considering image reconstruction capability of each individual moment and transform. The orthogonal properties of above mentioned moments along with the causes of their reconstruction error, numerical stability and invariance are described.**

Index Terms— **Zernike moments, pseudo Zernike moments, orthogonal Fourier Mellin moments, radial harmonic Fourier moments, Chebyshev-Fourier moments, polar harmonic transforms**

I. INTRODUCTION

The pioneering work of Hu in 1962 [1] on moment invariants, moments, and moment functions has opened many applications in the imaging field. Geometric moments (GMs) are one of the oldest moment based shape descriptors, which are used to generate a set of invariants that have been used in many pattern recognition applications [1]. Rotation invariant orthogonal moments and transforms (ORIMs and ORITs) are shape descriptors which are often used in many pattern recognition and image processing applications. The basis functions of these moments and transforms are orthogonal and complete, providing minimum information redundancy. The magnitude of the moments and transforms are rotation invariant. They are scale invariant because they are defined over a unit disk and their computation for an image is performed on the unit disk after coordinate mapping. The center of the unit disk is taken at the centroid of the image, therefore, they also become translation invariant. These characteristics are often referred to rotation, scale and translation (RST) invariant features. Amongst the various ORIMs are the three popular moments, Zernike moments (ZMs), pseudo Zernike moments (PZMs) and orthogonal Fourier-Mellin moments (OFMMs). The ZMs were first introduced to image analysis by Teague [2] in 1980. Teh and Chin [3] introduced PZMs, and OFMMs were first developed and introduced to image analysis by Sheng and Shen [4]. These moments have been applied successfully in many fields including, but not limited to, optical character recognition (OCR) [5,6], object recognition [7,8], pattern classification [9-12], content based image retrieval [13-15], image watermarking [16-18], palmprint verification [19], 2D/3D object recognition through sketches [20,21], rotation angle estimation, determination of image symmetry [22-24], image denoising [25] and image super resolution [26].

The ORIMs have been use in various image processing applications since 1980. On the other hand, ORITs have been

developed recently and hence their uses in various fields are being explored. They have characteristics similar to that possessed by ORIMs. However, they are less computation intensive. Among the various ORITs, There are two major transforms, namely, the radial harmonic Fourier moments (RHFMs) and polar harmonic transforms (PHTs). A major difference between the moments and transforms lies in the definition of radial part of the kernel function. The RHFMs were introduced by Ren et al. [27] in 2007. The PHTs which were developed by Yap et al. [28] in 2010 consists of three different transforms, namely, polar complex exponential transforms (PCETs), polar cosine transforms (PCTs), and polar sine transforms (PSTs). All three transforms are grouped under the name PHTs as the kernel of these transforms are harmonic in nature, that is, they are basic waves. The RHFMs have been used in various applications as given in [29,30]. Since PHTs are relatively new, their applications in various image processing tasks are being explored. They have been used in fingerprint classification [31], invariant image description [32], and image watermarking [33].

II. GEOMETRIC MOMENTS

GMs are one of the oldest moment based shape descriptors, which are used to generate a set of invariants that have been used in many pattern recognition applications. The geometric moments of order $(p+q)$ of image intensity function $f(x,y)$ are defined as [1]

$$G_{pq} = \int_{-\infty}^{\infty} \int_{-\infty}^{\infty} x^p y^q f(x,y) \, dx \, dy, \qquad (1)$$

The central moments are defined by

$$\mu_{pq} = \sum_{x=0}^{M-1} \sum_{y=0}^{N-1} (x-x_c)^p (y-y_c)^q f(x,y) \, dx \, dy, \qquad (2)$$

where

$$x_c = \frac{G_{10}}{G_{00}}, \; y_c = \frac{G_{01}}{G_{00}}, \qquad (3)$$

The normalized central moments, denoted by η_{pq}, are defined as

$$\eta_{pq} = \frac{\mu_{pq}}{\mu_{00}^{(p+q+2)/2}} \qquad (4)$$

The central moments are equivalent to the regular moments of an image that have been shifted such that the image centroid (x_c, y_c) is at the origin. As a result, central moments are invariant to translation of the image.
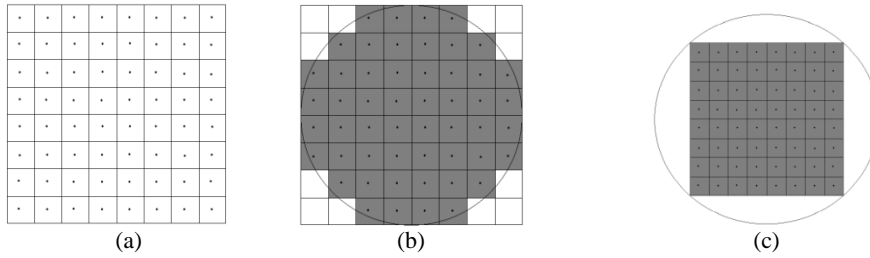
Fig.1: (a) An 8×8 image grid, (b) inscribed circle approximated by square grids, (c) outer circle containing the whole square image.

III. ORIMs AND ORITs

The ORIMs and ORITs of a continuous signal $f(x,y)$ over a unit disk are defined by

$$A_{pq} = \lambda \iint\limits_{x^2+y^2 \leq 1} f(x,y) V_{pq}^*(x,y)\,dxdy \qquad (6)$$

where λ is a normalizing factor which may depend on p. The function $V_{pq}^*(x,y)$ is the complex conjugate of the kernel function $V_{pq}(x,y)$ which is separable in the polar domain and has the form

$$V_{pq}(x,y) = R_{pq}(r)e^{jq\theta}, \qquad (7)$$

where, $r = \sqrt{x^2+y^2}$, $j = \sqrt{-1}$ and $\theta = \tan^{-1}(y/x)$, $\theta \in [0, 2\pi]$. The radial function $R_{pq}(r)$ is a polynomial in r for the ORIMs and for ORITs it is a harmonic function except for RHFMs.

One of the major characteristics of these moments and transforms is that their kernel function $V_{pq}(x,y)$ are orthogonal and complete. The orthogonality property yields

$$\iint\limits_{x^2+y^2 \leq 1} V_{pq}(x,y)V_{p'q'}^*(x,y)\,dxdy = \frac{1}{\lambda}\delta_{pp'}\delta_{qq'} \qquad (8)$$

where $\delta_{nm} = 1$, if $n = m$, and 0 otherwise

Owing to the property of orthogonality and completeness of the basis functions, the signal $f(x,y)$ can be represented as

$$\hat{f}(x,y) = \sum_{p_{min}}^{p_{max}} \sum_{q_{min}}^{q_{max}} A_{pq} V_{pq}(x,y) \qquad (9)$$

where p_{min}, q_{min}, p_{max} and q_{max} are the minimum and the maximum orders and repetitions used for computation. Larger are their values, the closer will be the reconstructed image $\hat{f}(x,y)$ to the given image $f(x,y)$.

III. COMPUTATIONAL FRAMEWORK

The ORIMs and ORITs defined by Eq.(6) pertain to a continuous signal $f(x,y)$ defined over unit disk. In digital image processing, the image function $f(i,k)$ is discrete and defined as a rectangular arrangement of pixels with i and k representing rows and columns, respectively. Let the image be a square image of size $N \times N$ pixels. A geometric transformation is performed which maps the $N \times N$ square grid into a unit disk.

$$x_i = \frac{2i+1-N}{D}, y_k = \frac{2k+1-N}{D}, \quad i,k = 0,1,2,...,N-1$$

$$\qquad (10)$$

$$D = \begin{cases} N & \textit{for inner disk} \\ N\sqrt{2} & \textit{for outer disk} \end{cases} \qquad (11)$$

The above transformation process is shown in Fig.1, where Fig.1(a) depicts an 8×8 pixel grid, Fig.1(b) represents its approximated form obeying the condition $x_i^2 + y_k^2 \leq 1$. The outer unit disk mapping enclosing the complete image is shown in Fig.1(c).

The ORIMs and ORITs are computed for a digital image using the above transformation as follows.

$$A_{pq} = \lambda \sum_{i=0}^{N-1} \sum_{\substack{k=0 \\ x_i^2+y_k^2 \leq 1}}^{N-1} f(x_i,y_k) \iint\limits_{p_{ik}} V_{pq}^*(x,y)\,dxdy \qquad (12)$$

where p_{ik} is the pixel area covered by the (i,k) pixel, i.e., $p_{ik} = \left[x_i - \frac{\Delta x}{2}, x_i + \frac{\Delta x}{2}\right] \times \left[y_k - \frac{\Delta y}{2}, y_k + \frac{\Delta y}{2}\right]$, with $\Delta x = \Delta y = 2/D$. It is difficult to find an analytical solution to the double integration, therefore, a zeroth order approximation is normally used. That is,

$$A_{pq} = \frac{4\lambda}{D^2} \sum_{i=0}^{N-1} \sum_{\substack{k=0 \\ x_i^2+y_k^2 \leq 1}}^{N-1} f(x_i,y_k) V_{pq}^*(x,y) \qquad (13)$$

The reconstructed image will exhibit very unstable behavior in the center of the image. Along the boundary of the image, its behavior is similar to the other three ORITs. The harmonic function $e^{-jq\theta}$ changes rapidly within a pixel, when either q increases or in the neighborhood of the center of the image. Therefore, the computation error associated with the harmonic function affects the central pixels more than those of the surrounding areas as q increases. The rate of change of the function over a pixel area will affect the accuracy of their computation. Higher is the rate of change in a certain region, the more inaccurate will be the moments and transforms. Consequently, the moments and transforms will be computed more accurately whose kernel functions have a smaller magnitude of the rate of change. As a result of this trend, the ZMs are the most stable ones among the three moments which is also demonstrated by the quality of the reconstructed images.

p_{max}	ZMs	PZMs	OFMMs ($q_{max=}$ p_{max})	PCETs ($q_{max=}$ p_{max})	PCTs ($q_{max=}$ p_{max})	PSTs ($q_{max=}$ p_{max})	RHFMs ($q_{max=}$ p_{max})
10	$\varepsilon=0.063610$	$\varepsilon = 0.042737$	$\varepsilon = 0.039192$	$\varepsilon= 0.031957$	$\varepsilon = 0.037413$	$\varepsilon = 0.081428$	$\varepsilon= 0.048093$
20	$\varepsilon=0.034770$	$\varepsilon = 0.02656$	$\varepsilon=0.278552$	$\varepsilon= 0.238613$	$\varepsilon = 0.020717$	$\varepsilon =0.039026$	$\varepsilon=0.084605$
30	$\varepsilon=0.045693$	$\varepsilon = 0.032295$	$\varepsilon = 1.204952$	$\varepsilon= 0.959409$	$\varepsilon = 0.047243$	$\varepsilon = 0.039700$	$\varepsilon= 0.302110$
40	$\varepsilon=0.100708$	$\varepsilon = 0.06507$	$\varepsilon =4.59407$	Distorted image	$\varepsilon = 0.550076$	$\varepsilon = 0.472324$	$\varepsilon=1.126026$
50	$\varepsilon=0.392099$	$\varepsilon = 0.089781$	$\varepsilon =17.545450$	Distorted image	$\varepsilon = 1.328942$	$\varepsilon = 1.205462$	$\varepsilon=3.617752$
60	$\varepsilon=0.717576$	$\varepsilon = 0.147445$	$\varepsilon =26.82387$	Distorted image	Distorted image	Distorted image	$\varepsilon=9.701388$
70	$\varepsilon=1.029269$	$\varepsilon = 0.238981$	$\varepsilon =39.87098$	Distorted image	Distorted image	Distorted image	Distorted image

Fig.2: Reconstructed Lena image of 64×64 pixels using zeroth order approximation of various ORIMs and ORITs for different values of $p_{\max}$ and $q_{\max}$.

IV. CONCLUSIONS

There are a number of circularly orthogonal radial moments and radial harmonic transforms that are rotation invariant. These moments and transforms are made scale invariant when they are computed in a unit disc. Due to their unique characteristics of being rotation and scale invariant, these moments and transforms have been used in various image processing applications. However, because of the discrete nature of the image function $f(x, y)$, these characteristics are severely affected during the implementation of the moments and transforms. Moreover the image reconstruction ability and numerical stability of these moments and transforms varies significantly. These issues have been analyzed in great details in this paper and the results are concluded as follows.

1. Among all moments and transforms the *ZMs* are the most stable ones which have the best image reconstruction capability and rotation and scale invariance.

2. The *PZMs* have best image reconstruction capability for low orders of moment which even surpasses the performance of *ZMs* at low orders, $p_{\max} \leq 20$. At low orders of moments the rotation and scale invariance of *PZMs* is marginally better than that of *ZMs*, the performance of *ZMs* becomes better when $p_{\max} > 20$.

3. A peculiar behavior was observed for all moments and transforms except for *ZMs*, in image reconstruction at the centre of the image at which the reconstructed image function value was observed to be abnormally high. In the case of *PSTs* the image function values were very low in the neighborhood of the centre of the image.

REFERENCES

1. M. K. Hu, Visual pattern recognition by moment invariants, IEEE Trans. Inf. Theory. IT 8 (1962) 179-187.

2. M. R. Teague, Image analysis via the general theory of moments, J. Opt. Soc. Am. 70(8) (1980) 920-930.

3. C.-H. Teh, R. T. Chin, On image analysis by the methods of moments, IEEE Trans. Pat. Anal. Mach. Intell. 10 (4) (1988) 496-513.

4. Y. Sheng, L.Shen, Orthogonal Fourier Mellin moments for Invariant Pattern Recognition, IEEE Trans. J. Opt. Soc. Am., 11 (6) (1994) 1748-1757.

5. C. Kan, M. D. Srinath, Invariant character recognition with Zernike and orthogonal Fourier-Mellin moments, Pattern Recognition 35 (2002) 143-154.

6. A. Broumandnia, J. Shanbehzadeh, Fast Zernike Wavelet moments for Farsi character recognition, Image and Vision Computing 25 (2007) 717-729.

7. A. Khotanzad, J.-H. Lu, Classification of invariant image representations using a neural network, IEEE Trans. Acoust., Speech, Signal Process. 38 (1990) 1028–1038.

8. G.A. Papakostas, Y.S. Boutalis, D.A. Karras, B.G. Mertzios, A new class of Zernike moments for computer vision applications, Information Sciences 177 (2007) 2802–2819.

9. L. Wang, G. Healey, Using Zernike moments for the illumination and geometry invariant classification of multispectral texture, IEEE Trans. Image Process. 7 (2) (1998) 196–203.

10. P. Raveendran, S. Omatu, Performance of an optimal subset of Zernike features for pattern classification, Information Sciences 1 (3) (1994) 133-147.

11. C.-Y. Wee, R. Paramesran, F. Takeda, New computational methods for full and subset Zernike moments, Information Sciences 159 (2004) 203–220.

12. Z. Chen, S.-K. Sun, A Zernike moment phase descriptor for local image representation and matching, IEEE Trans. On Image Process. 19 (1) (2010) 205-219.

13. Y.-S. Kim, W.-Y. Kim, Content-based trademark retrieval system using visually salient features, In: Proceedings of 1997 IEEE Computer Society Conference on Computer Vision and Pattern Recognition (1997) pp. 307–312.

14. S. Li, M.-C. Lee, C.-M. Pun, Complex Zernike moments features for shape based image retrieval, IEEE Trans. Systems, Man, and Cybernetics-Part A: Systems and Humans 39 (1) (2009) 227-237.

15. C. Singh, Pooja, Improving image retrieval using combined features of Hough transform and Zernike moments, Optics and Lasers in Engineering 49 (2011) 1384–1396.

16. Y. Xin, S. Liao, M. Pawlak, Circularly orthogonal moments for geometrically robust image watermarking, Pattern Recognition 40 (2007) 3740-3752.

17. H. S. Kim, H. K. Lee, Invariant image watermarking using Zernike moments, IEEE Trans. Image Processing 13 (8) (2003) 766-775.

18. E. D. Tsougenis, G. A. Papakostas, D. E. Koulouriotis, V. D. Tourassis Performance evaluation of moment-based watermarking methods: A review, The Journal of Systems and Software (2012).

19. Y. H. Pang, A. B. J. Teoh, D. C. L., Ngo, F. S. Hiew, Palmprint verifications with moments, J. WSCG 12 (2003) 1-3.

20. T. F. Ansary, M. Daoudi, and J.-P. Vandeborre, A Bayesian 3D search engine using adaptive views clustering, IEEE Trans. Multimedia 9 (1) (2007) 78-88.

21. S. Hou and K. Ramani, Calligraphic Interfaces: Classifier combination for sketch-based 3D part retrieval, Computers and Graphics 31(4) (2007) 598-609.

22. W-Y. Kim and Y-S Kim, Robust rotation angle estimator, IEEE Trans. on Pattern Analysis and Machine Intelligence 21(8) (1999) 768-773.

23. N. Bissantz, H. Holzmann, M. Pawlak, Testing for image symmetries-with application to confocal microscopy, IEEE Trans. On Information Theoy 55 (4) (2009) 1841-1855.

24. J. Revaud, G. Lavoue, A. Baskurt, Improving Zernike moments comparison for optimal similarity and rotation angle retrieval, IEEE Trans Pattern Anal Mach Intell. 31 (4) (2009) 627-636.

25. Z. Ji, Q. Chen, Q.-S. Sun, D.-S. Xia, A moment-based nonlocal-means algorithm for image denoising, Information Processing Letters 109 (2009) 1238–1244.

26. X. Gao, Q. Wang, X. Li, D. Tao, K. Zhang, Zernike moment-based image super resolution, IEEE Transactions on Image Proc. 20 (10) (2011) 2738-2747.

27. H. Ren, A. Liu, J. Zou, D. Bai and Z. Ping, Character reconstruction with radial harmonic Fourier moments, in Proc. of the 4th Int. Conf. on Fuzzy Systems and Knowledge Discovery 2007 (FSKD07), 3 (2007) 307-310.

28. P.T. Yap, X. Jiang, A.C. Kot, Two dimensional polar harmonic transforms for invariant image representation, IEEE Trans. Pat. Anal. Mach. Intell., 32 (7) (2010) 1259-1270.

29. C. Singh, R. Upneja, A Computational Model for Enhanced Accuracy of Radial Harmonic Fourier Moments, Presented in "Proceedings of World Congress of Engineering 2012 Vol II, WCE 2012, July 4-6, London, U.K.

30. C. Singh, S.K. Ranade, A high capacity image adaptive watermarking scheme with radial harmonic Fourier moments, Digital Signal Processing (2013).

31. M. Liu, X. Jiang, A.C Kot, P.T. **Yap,** Application of polar harmonic transforms to fingerprint classification, in Chen, C.H. (Ed.): Emerging Topics in Computer Vision and its Applications, World Scientific Publishing, 2011.

32. T.V. Hoang, S. Tabbone, Generic polar harmonic transforms for invariant image description, IEEE ICIP, Brussels, Belgium, Sep 2011, pp. 845-848.

33. L. Li, S. Li, A. Abraham, J.-S. Pan, Geometrically invariant image watermarking using polar harmonic transforms, Information Sciences (2012).

34. R.C. Gonzalez, R.E. Woods, Digital Image Processing, 3rd Edition, Prentice Hall, 2008